

PAPER • OPEN ACCESS


Sequence of penalties method to study excited states using VQE

To cite this article: R Carobene *et al* 2023 *Quantum Sci. Technol.* **8** 035014

View the [article online](#) for updates and enhancements.

You may also like

- [Improving the accuracy and efficiency of quantum connected moments expansions](#)
Daniel Claudino, Bo Peng, Nicholas P Bauman et al.
- [Many-body calculations for periodic materials via restricted Boltzmann machine-based VQE](#)
Shu Kanno and Tomofumi Tada
- [Faster variational quantum algorithms with quantum kernel-based surrogate models](#)
Alistair W R Smith, A J Paige and M S Kim

 **kiutra**

Easy-to-use and Helium-3 free
cryogenics solutions

LEARN MORE

Quantum Science and Technology



PAPER

Sequence of penalties method to study excited states using VQE

OPEN ACCESS

RECEIVED
31 August 2022

REVISED
6 April 2023

ACCEPTED FOR PUBLICATION
2 May 2023

PUBLISHED
15 May 2023

Original Content from
this work may be used
under the terms of the
[Creative Commons
Attribution 4.0 licence](#).

Any further distribution
of this work must
maintain attribution to
the author(s) and the title
of the work, journal
citation and DOI.



R Carobene^{1,*} , S Barison² and A Giachero^{1,3,4}

¹ Dipartimento di Fisica, Università di Milano-Bicocca, I-20126 Milano, Italy

² Institute of Physics, École Polytechnique Fédérale de Lausanne (EPFL), CH-1015 Lausanne, Switzerland

³ Bicocca Quantum Technologies (BiQuTe) Centre, I-20126 Milano, Italy

⁴ INFN—Sezione di Milano Bicocca, I-20126 Milano, Italy

* Author to whom any correspondence should be addressed.

E-mail: r.carobene@campus.unimib.it

Keywords: VQE, quantum computing, quantum simulation, excited states

Abstract

We propose an extension of the variational quantum eigensolver (VQE) that leads to more accurate energy estimations and can be used to study excited states. The method is based on the introduction of a sequence of increasing penalties in the cost function. This approach does not require circuit modifications and thus can be applied with no additional depth cost. Through numerical simulations, we show that we are able to produce variational states with desired physical properties, such as total spin and charge. We assess its performance both on classical simulators and on currently available quantum devices, calculating the potential energy curves of small molecular systems in different physical configurations. Finally, we compare our method to the original VQE and to another extension, obtaining a better agreement with exact simulations for both energy and targeted physical quantities.

1. Introduction

In recent years, the development of quantum computing hardware made strides from the first working prototypes to devices with more than a hundred qubits [1]. Companies such as IBM and Google have revealed plans to build thousands or even a million qubits devices by the end of the decade. However, it has to be highlighted that the number of qubits is not the only metric to take into account in a quantum computing platform and the current amount of operations that can be performed is strongly limited by hardware noise and decoherence. While quantum error correction schemes have been proposed and even tested on hardware [2–6], their large-scale application remains still far in the future.

In order to provide meaningful results in the near-term, hybrid algorithms that combine quantum devices with classical computers have been proposed [7–17]. In these schemes a quantum computer is only in charge of a subroutine, while the classical computer governs the whole algorithm. This greatly reduces the number of quantum operations required and those methods have been demonstrated to be naturally robust with respect to certain hardware errors [18].

One such scheme is the variational quantum eigensolver (VQE) [19, 20], where a parameterized quantum circuit is used to approximate the ground state of an interacting quantum system. In this case a quantum computer is used to measure the energy and its derivatives, then a classical optimizer will tune the variational parameters according to those. VQE has been widely studied and extended to improve the final result precision or to lower the hardware requirements [21–24].

More recently, extensions of VQE to the study of excited states have been proposed. As an example, in the quantum subspace expansion method [25], excitation operators are applied to the variational ground-state, while the quantum imaginary time evolution algorithm [10] can be used to construct the Lanczos subspace [26]. Alternatively, one can directly compute excitation energies using the quantum equation of motion method [11], or even use algorithms of quantum machine learning [27]. Finally, another category of VQE

variants is based on the idea of modifying the cost function to guide the optimization to the desired state [28–33].

In this paper, we expand on the last approach and propose a method based on the introduction of a sequence of increasing penalties in the cost function that leads to better approximated eigenstates and can be used to study excited states. We chose to name our algorithm sequence of penalties VQE (SPVQE). Based on a cost function modification, the proposed method does not need more resources than VQE.

The structure of this paper is as follows: in section 2 we review the VQE algorithm, its constrained modification, the constrained variational quantum eigensolver (CVQE), and present the SPVQE method, while in section 3 we apply it to the study of excited and ionized state of small chemical compounds, assessing the performances both on classical simulators and on real hardware. Finally, section 4 concludes the paper with some considerations and outlooks on the proposed method.

2. Methods

2.1. VQE

Here we briefly review the VQE, for a more detailed explanation we suggest to refer to [18, 19].

Consider a physical system described by the Hamiltonian H . The aim of the VQE is to prepare a variational ground state approximation of this system on a quantum computer. First, the Hamiltonian is mapped into a Pauli operator [34–36], in order to be able to measure expectation values on quantum hardware. Then, the qubits are prepared in the state $|\psi(\theta_0)\rangle = V(\theta_0)|0\rangle$, where $V(\theta)$ is a combination of parameterized quantum operations (gates) depending on the set of parameters θ , and θ_0 is the initial choice of parameters.

We use the quantum device to measure the expectation value of H , defined as $E(\theta) = \langle\psi(\theta)|\hat{H}|\psi(\theta)\rangle$, and its derivatives with respect to the parameters θ [37–40]. Finally, we feed these quantities to a classical optimizer that determines new values of θ in order to decrease $E(\theta)$. When this iterated procedure converges, we obtain a set of parameters θ^* that defines the desired state.

Now suppose that, given some operator \hat{A} , we want to prepare the eigenstate corresponding to its eigenvalue a . Given that these configurations may not correspond to the ground state of the system, we cannot rely solely on lowering the energy.

More generally, we may be interested in studying an excited state in a region in which quantum states with different physical properties have similar energies. In all these cases, VQE may fail to correctly approximate the desired state.

In perspective of using VQE to study molecules with complex energy spectra, we must develop a robust method that preserves every physical property we may desire to fix.

2.2. Constrained variational quantum eigensolver (CVQE)

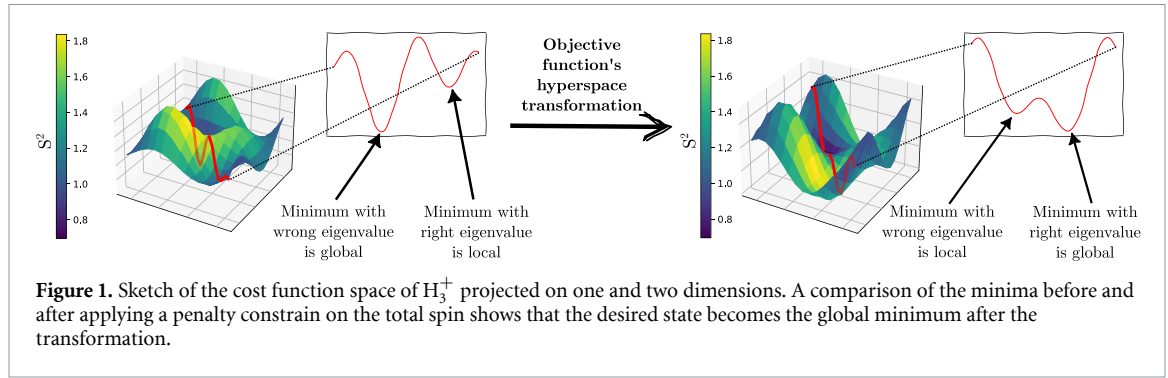
Some of the proposed variations of VQE already include in the optimization process information about additional operators [41–43]. In particular, we will briefly recall the CVQE [29].

While in the standard VQE approach we minimize the energy as stated in section 2.1, the CVQE method introduces a redefined cost function $F(\theta)$ by adding a penalty multiplier for each of the operators we may desire to fix:

$$F(\theta, \mu) = \langle\psi(\theta)|\hat{H}|\psi(\theta)\rangle + \sum_i \mu_i \left[\langle\psi(\theta)|\hat{A}_i|\psi(\theta)\rangle - a_i \right]^2 \quad (1)$$

here \hat{A}_i with $i \in \{1, \dots, m\}$ is a set of operators, μ_i are their corresponding multipliers and a_i the eigenvalues that we want to fix. Chosen μ_i sufficiently large, the desired state will correspond to a global minimum of the cost function. In figure 1 we show as an example the variational landscape computed for the H_3^+ molecule, obtained by scanning the Hamiltonian and the spin operator on two random parameters. We see that the desired state is transformed from a local to a global minimum through the application of the constrain. We highlight that, among all the possible states satisfying the given constraints, the global minima will be always the lowest energy state. For this reason, we envision the combination of our method with other algorithms, such as the quantum subspace expansion [25] or the quantum equation of motion [11], to provide even more accurate estimations of excited state properties of physical systems.

In a practical usage of CVQE, however, the combination of an unknown good starting point θ_0 and restricted local knowledge of the loss landscape often leads to convergence into local minima. Moreover, a careful fine tuning of μ_i is often required since multipliers too large yield to narrow global minima, while multipliers too small do not highlight sufficiently the global minima with respect to local ones.



2.3. SPVQE

We propose a simple, yet effective, variation of CVQE: the SPVQE.

We want to have a penalty large enough to exclude any local minima, while avoiding changing the cost function space too rapidly. Therefore, we propose to repeat the constrained optimization increasing penalty multipliers by steps [44].

For clarity of exposition, we will constrain a single operator. The method can be extended to multiple constraints modifying the penalty term.

First, we choose the maximum value of the penalty multiplier (μ_{\max}) and the number of steps N_s . If the gap between the desired state energy E and the ground state one (E_{GS}) is approximately known, we can choose the value of μ_{\max} so that it satisfies the inequality [45]:

$$\mu_{\max} \geq \frac{E_{GS} - E}{\left(\langle \psi_{GS} | \hat{A} | \psi_{GS} \rangle - a\right)^2}. \quad (2)$$

It is possible to obtain an estimation of the gap by using classical approximated methods. Even if this classical estimation does not reach chemical accuracy, it provides an idea of the magnitude of the gap. In general, N_s and μ_{\max} are hyperparameters of the SPVQE method, therefore there is not a rigorous framework to exactly set the parameters and we have to rely on heuristics.

Equation (2) provides a lower limit for the maximum multiplier, but we do not have an upper limit for the single step multiplier and therefore there is no guarantee that the choice made will leads to the feasible region. In a theoretical perspective, μ_{\max} can be chosen arbitrarily large since N_s compensates for the narrowing of the global minimum, hence the problem is reduced to the choice of N_s .

In practice, we can first set N_s by considering how much time we can afford on the quantum platform, given that computational time grows linearly with N_s . In our examples a number of steps of ≈ 10 was always sufficient, as we will show in figure 4.

We run N_s instances of VQE constrained with increasing penalties. At each iteration $k \in \{1, \dots, N_s\}$, we compute the penalty using $\mu = \frac{\mu_{\max} * k}{N_s}$, using the optimal set of parameters θ_{k-1}^* of the previous step as starting point. Finally, the best loss computed over all the iterations is returned as the result.

The complete method is schematically presented in algorithm 1.

Algorithm 1 Sequence of penalties VQE.

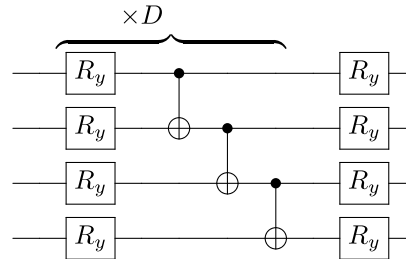
- 1: Given a random starting point θ_0 and a Hamiltonian \hat{H}
 - 2: Chosen a μ_{\max} and a number of iteration N_s
 - 3: We define $s = \mu_{\max}/N_s$
 - 4: Given, initially: $\mu = 0$
 - 5: **for** $k = 1, 2, 3, \dots, N_s$ **do**
 - 6: Penalty term: $P = \mu \left(\langle \psi(\theta) | \hat{A} | \psi(\theta) \rangle - a \right)^2$
 - 7: Define cost function: $F = \langle \psi(\theta) | \hat{H} | \psi(\theta) \rangle + P$
 - 8: Start VQE with parameters θ_{k-1}^*
 - 9: Save θ_k^*
 - 10: Update the multiplier: $\mu \leftarrow \mu + s$
 - 11: **end for**
- return** Energy correspondent to minimum cost function ($E = F - P$)
-

2.4. Numerical simulations

To demonstrate a practical SPVQE application, we considered molecular systems where the constrained operators were the particle number or the total spin operator:

$$\hat{A} \in \{\hat{S}^2, \hat{N}\}. \quad (3)$$

We chose a hardware efficient ansatz composed by a layer of single qubit rotations R_y , each one with an independent parameter, followed by an entangling layer of CNOTs. This structure is repeated D times and, at the end of the circuit, another layer of R_y rotations is applied. As an example, for 4 qubits the circuit reads



In the following experiments we set $D = 3$, unless where explicitly stated. To limit the number of qubits required, we considered a minimal Slater-type orbital basis set constructed with six primitive Gaussian orbitals (STO-6G) [20, 23]. The qubit mapping of the Hamiltonian is done with parity mapping [35] with the two qubit reduction. For noiseless simulations we used the SciPy conjugate gradient optimizer [46]; whereas for noisy simulations and hardware calculations we used the Nakanishi–Fujii–Todo optimizer [47] that proved to give the best results.

Some final measurements were performed after the VQE procedure to improve results in noisy simulations and hardware calculations. These are presented in appendix A. The simulations and quantum hardware computations that can be found in section 3 and in the appendices are performed using IBM's open source library *Qiskit* [48].

3. Results

In this section we will use the SPVQE algorithm to find ground and excited states of molecular systems and compare the results to VQE and CVQE calculations. In particular, we will consider the Born–Oppenheimer approximation of molecular Hamiltonians, that in second quantization have the form

$$\hat{H} = \sum_{ij} h_{ij} \hat{a}_i^\dagger \hat{a}_j + \frac{1}{2} \sum_{ijkl} g_{ijkl} \hat{a}_i^\dagger \hat{a}_k^\dagger \hat{a}_l \hat{a}_j + E_0, \quad (4)$$

where \hat{a}_i^\dagger and \hat{a}_i are fermionic creation and annihilation operators corresponding each to a different spin-orbital and the coefficients h_{ij} and g_{ijkl} are coefficient accounting for electron kinetic energy, interactions electrons–nuclei and electron–electron repulsion. E_0 is the shift obtained by fixing the atomic positions and calculating their repulsion energy.

Details on the systems studied can be found in appendix D, while complete results including nuclear repulsion energy, frozen core energy and parameters obtained at every step are available on [49].

3.1. Using SPVQE to study excited states

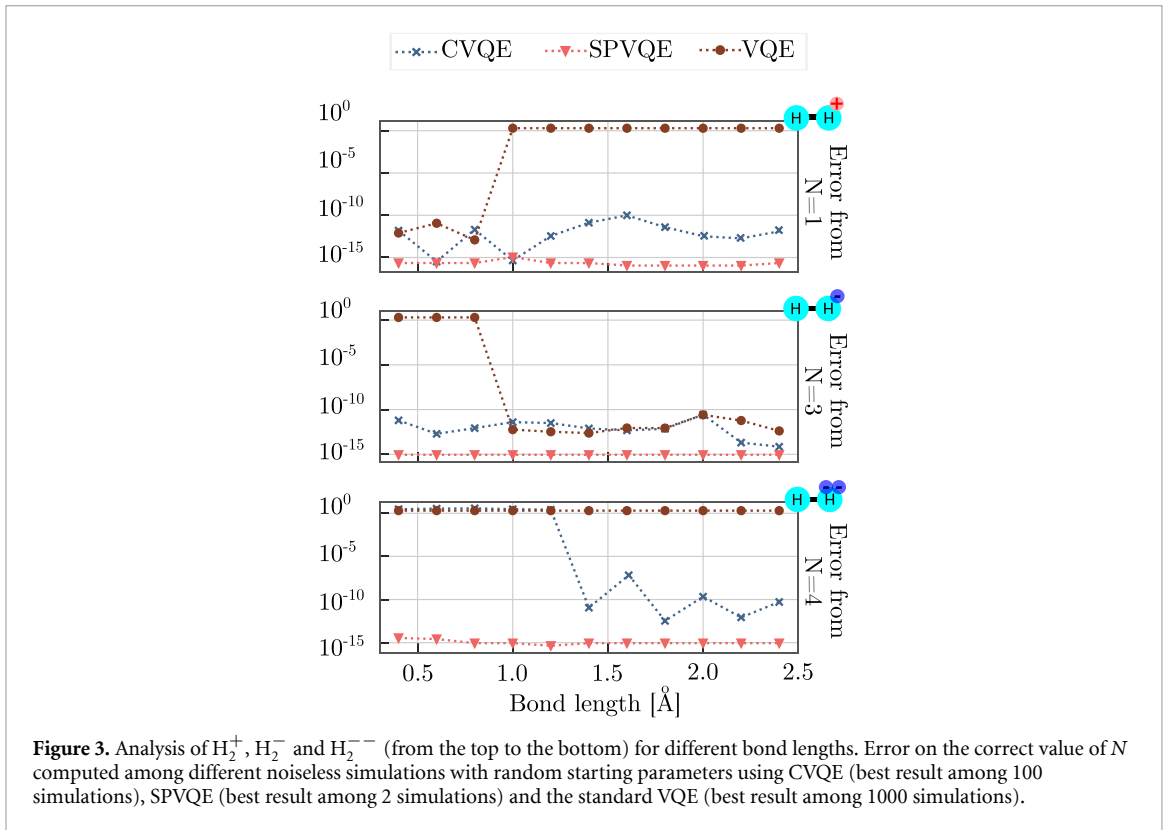
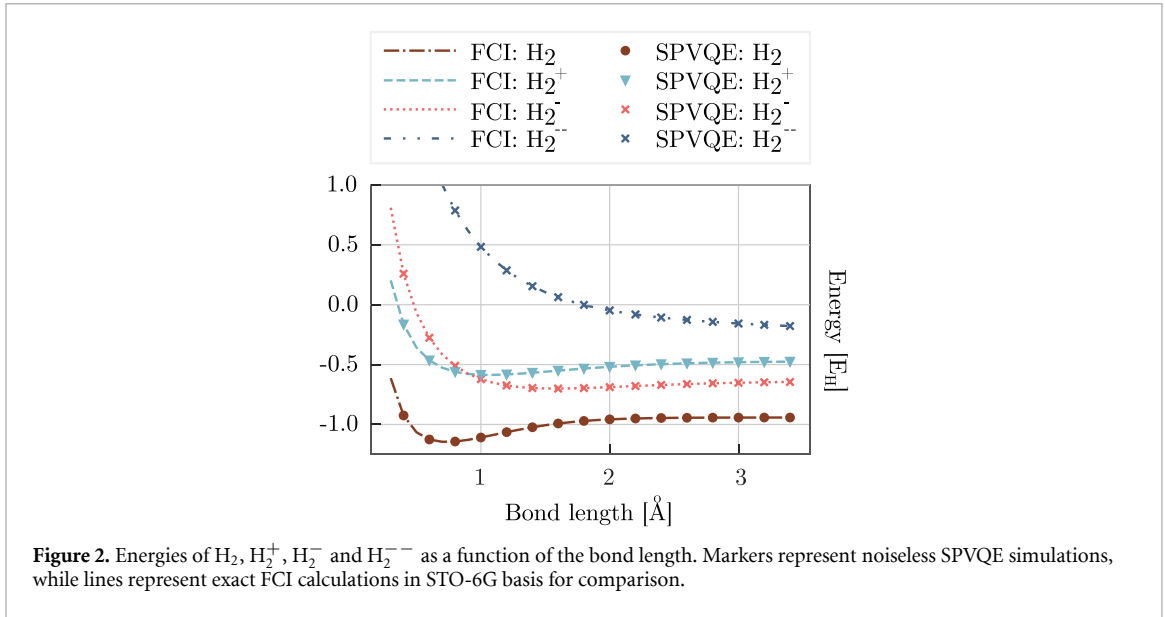
First, to assess the performance of the SPVQE algorithm, we studied the energies of the first ionic states of H_2 defined by different particles numbers, namely H_2^+ ($N = 1$), H_2^- ($N = 3$) and H_2^{2-} ($N = 4$). We analyzed the energy of the molecules in different atomic configurations, varying the bond length from 0.3 Å to 3.5 Å.

Calculations were performed on a classical computer simulating a noiseless quantum environment. The circuit describing H_2 and its excited states needs two qubits, for a total of eight parameters when a $D = 3$ circuit is considered.

The dissociation profiles computed with SPVQE are presented in figure 2 and compared to the numerically exact solutions obtained with the classical full configuration interaction method [50].

In all simulations presented in figure 2 SPVQE is able to target the physically correct state among the various ones that are present.

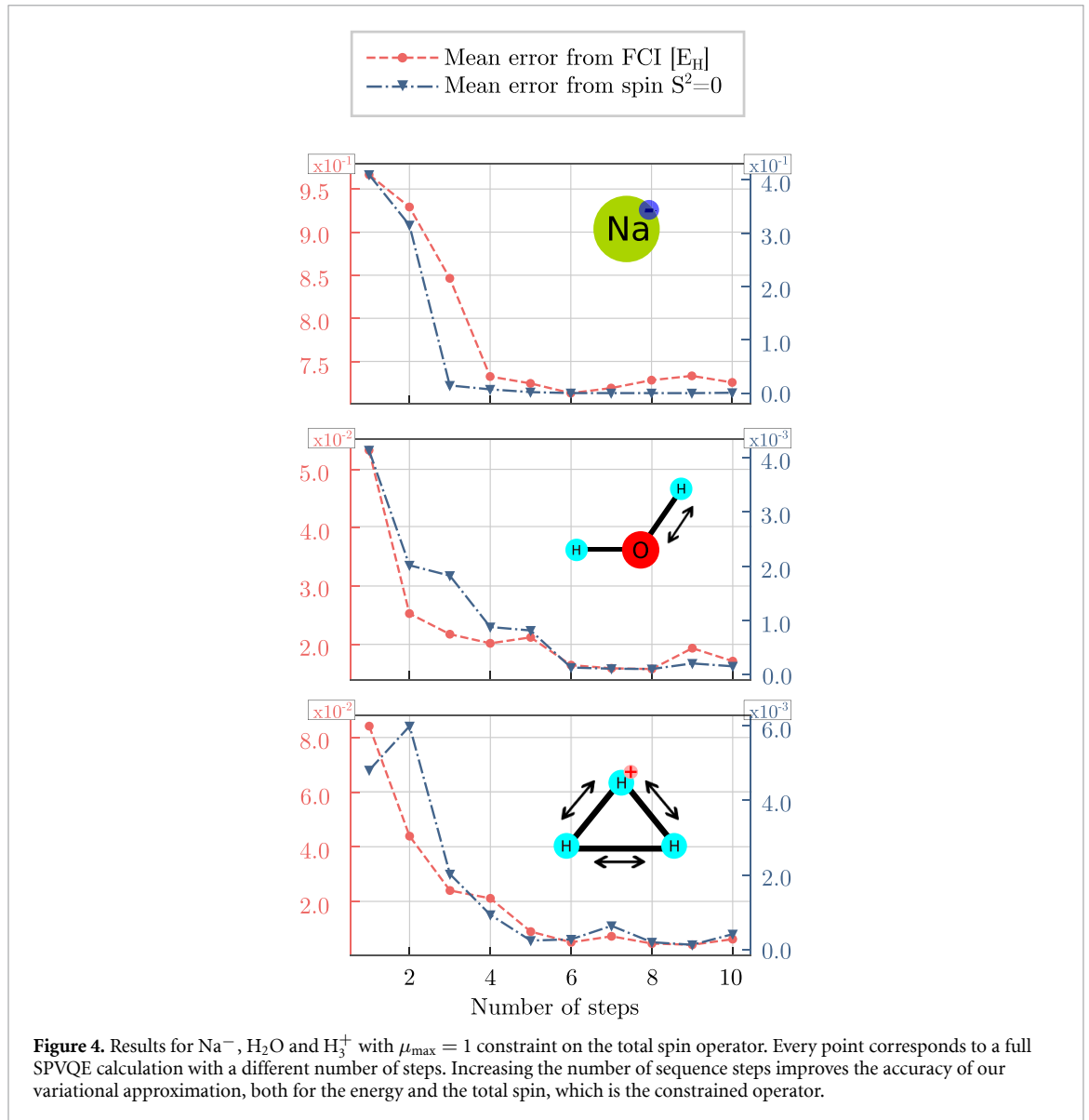
Then, we repeated these simulations using CVQE and VQE and show a comparison of the different methods in figure 3. VQE points correspond to the best value obtained among 1000 simulations with random starting parameters. CVQE simulations were repeated 100 times and SPVQE calculations 2 times.



The standard VQE algorithm struggles to find a good approximation for every configuration. In particular, it swaps H_2^+ and H_2^- taking the state with the lowest energy between them (for that specific bond length) and is never able to approximate H_2^{--} that has a much higher energy. CVQE reaches good results for both H_2^+ and H_2^- . However, for H_2^{--} it needs a higher penalty (in particular at low bond lengths) and this misleads the algorithm that fails to find the correct minimum. Lastly, SPVQE reaches the correct state at every configuration, hitting machine precision.

3.2. Dependence on the number of steps

In this section we analyze the performance of SPVQE as a function of the number of sequence steps N_s . In figure 4, we show the results for three different molecules: Na^+ , H_2O and H_3^+ .



While H_2O is not an excited state, the addition of a constraint is still needed because the molecule has an excited level with a very similar energy, making the convergence of standard VQE to a state with the right physical properties difficult [23, 29].

For H_2O we varied the length of one of the H – O bond from 1 Å to 3 Å, while for H_3^+ we varied the length of all H – H bonds from 1 Å to 3 Å. These configurations are difficult to handle for the standard VQE, which is not able to reach a correct approximation.

For Na^- and H_2O the simulations were carried in the active space, freezing core orbitals to diminish the number of needed qubits. This resulted in an ansatz with 24 parameters on 6 qubits for Na^- , considering 2 electrons in the 4 most external molecular orbitals, and one with 16 parameters on 4 qubits for H_2O , considering just 4 electrons in 3 orbitals. H_3^+ simulations are performed without frozen core approximation, requiring 4 qubits and 16 parameters. Thus, every marker on the graphs represents the average result obtained considering a SPVQE iteration for each ionic configuration.

The plots show that even with few iterations of the SPVQE method, the total spin is correctly constrained to the desired value, while the energy decreases accordingly. We note that the first marker of each graph, namely the single-step optimization, is equal to a CVQE calculation.

3.3. Robustness against starting point choice

Finding the ground state of a quantum system is a hard problem even on quantum computers [51]. For this reason, VQE and its modifications are not guaranteed to reach the global minimum of the energy (or the

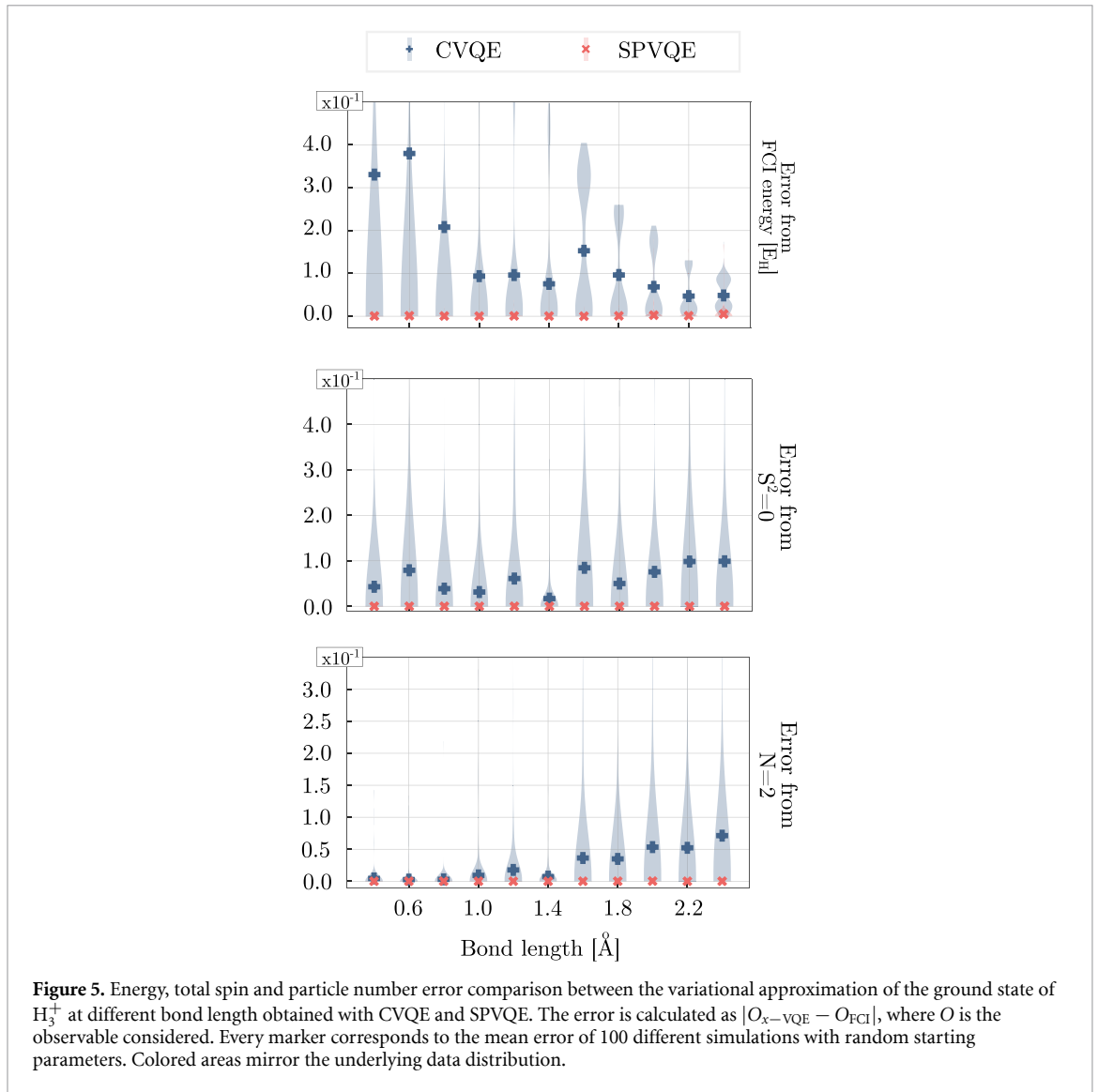


Figure 5. Energy, total spin and particle number error comparison between the variational approximation of the ground state of H_3^+ at different bond length obtained with CVQE and SPVQE. The error is calculated as $|O_{x-VQE} - O_{FCI}|$, where O is the observable considered. Every marker corresponds to the mean error of 100 different simulations with random starting parameters. Colored areas mirror the underlying data distribution.

modified cost function) in polynomial time in every scenario. The convergence of the algorithm depends on different factors. The choice of starting parameters is one of them and can hinder the convergence of the algorithm. Despite this importance, often we do not have the possibility to make an educated guess on the starting set of parameters; thus a certain robustness with respect to the choice of the starting parameters is desired.

In this section we analyze the robustness of SPVQE and compare it to CVQE. To this aim, we performed multiple simulations of the H_3^+ molecule for bond lengths varying from 0.4 Å to 2.5 Å. Results of these calculations are shown in figure 5. Every marker is obtained considering multiple simulations with random starting parameters and represents the mean error of the computed energies, numbers of particle, spins. The colored areas of the *violin-plot* mirror the underlying data distribution.

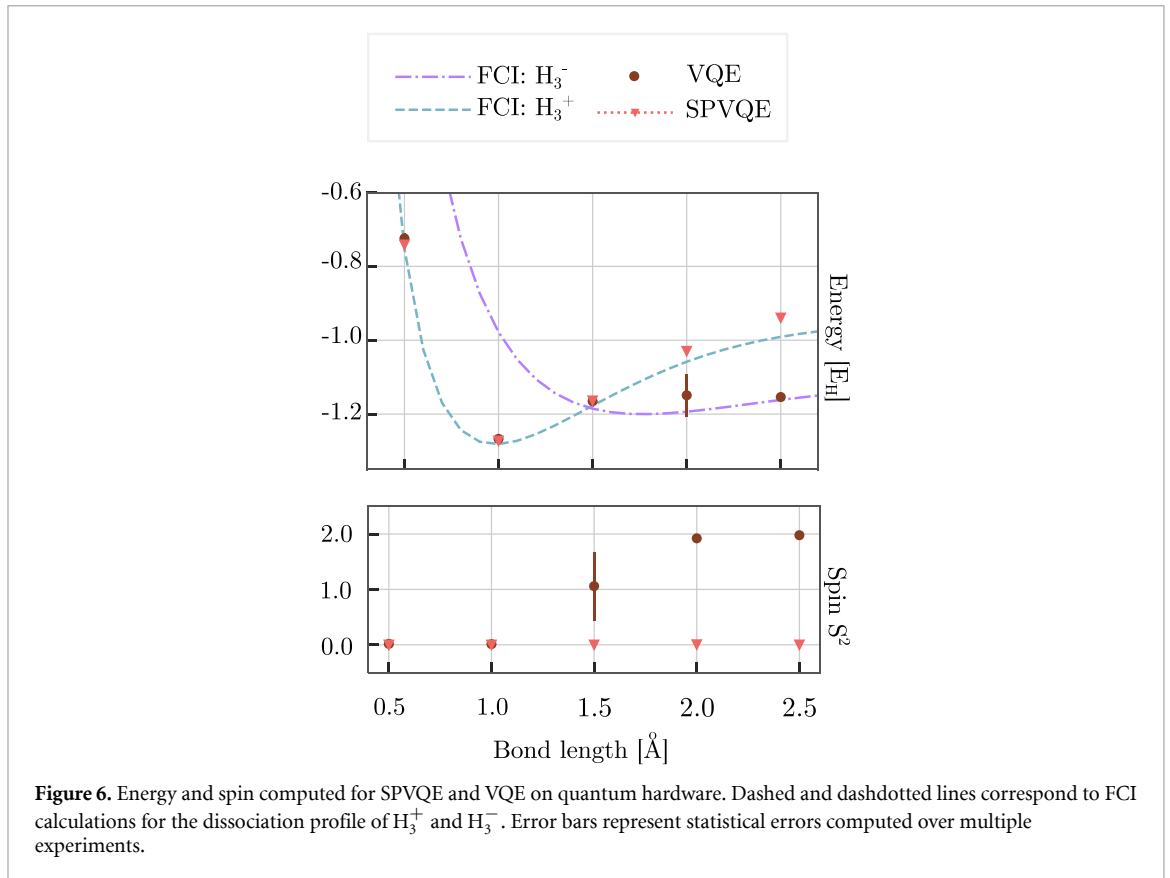
SPVQE proves to be more robust in every analyzed situation, with lower errors and smaller deviations from the mean value. This is due to the fact that SPVQE is generating itself a sequence of improving educated guesses.

To show that this effect is not due to some inherent property of the H_3^+ molecule, in appendix B we report the calculations performed on different chemical systems.

3.4. Hardware experiments

Finally, we tested SPVQE on real quantum hardware, using the IBM Quantum processor *ibmq_quito*.

We analyzed the trihydrogen cation (H_3^+) for bond lengths varying from 0.3 Å to 2.5 Å. A standard VQE approach works properly for bond lengths smaller than ≈ 1.5 Å: after that point, the energy of H_3^+ gets lower



than the desired configuration, making the algorithm converge to the wrong minimum. Thus, the optimization process fails to preserve the particles number (it finds a state where $N = 4$) and also the spin (it computes $S^2 = 1$). Therefore we chose to constrain $S^2 = 0$.

As we stated before, current quantum hardware has limited performances and requires extreme care to reduce errors impact. Since *ibmq_quito* has a medium-low quantum volume [52] of 16, we reduced the depth of the ansatz described in section 2.4 choosing $D = 2$. Once the circuit is transpiled using *ibmq_quito* basis gates {CX, ID, RZ, SX, X}, its final depth is 19. For every bond length configuration we performed 4 independent calculations with 1024 shots each. Starting parameters have been chosen randomly.

Hardware experiments were prepared simulating the SPVQE algorithm in a noisy environment. The obtained results, reported in appendix C, confirmed us that SPVQE could maintain the desired advantages even in the presence of noise.

Hardware results are showed in figure 6.

We can see that the profile computed using SPVQE correctly approximate the exact calculated one. VQE fails to correctly approximate the state of H_3^+ at high bond distance, when H_3^- energy level became lower than the H_3^+ one. Error bars correspond to the standard deviation obtained among the four different results and thus represent the statistical error.

VQE shows the biggest statistical uncertainty at 2 Å. For this configuration, the VQE wave functions always present the wrong spin. Therefore, this point can be interpreted as corresponding to a molecular configuration where it is difficult to find the global minimum of the Hamiltonian.

Looking at the lower panel of figure 6, we see that SPVQE is able to constrain S^2 to the desired value even on hardware, while VQE starts to miscalculate it at 1.5 Å, where the energies of the two different spin configurations are similar. Moreover, the distance where the energies of H_3^+ and H_3^- are almost equal has the

biggest statistical uncertainty on the spin. This can be explained by the fact that VQE just minimizes the energy, thus finding a state not characterized by a precise spin, but rather by a mixed spin state.

4. Discussion

In this paper we introduced a simple, yet effective, modification of the VQE algorithm to enable excited and ionized state simulations. The proposed method, SPVQE, was tested for small molecules both on classical simulators and on real quantum hardware and proved to work correctly in the studied cases. Moreover, the algorithm showed an increased robustness against the choice of the starting point. For these reasons, we envision to use SPVQE in combination with other methods to study excited states of physical systems with higher accuracy on quantum computers.

The choice of the parameters, number of iterations and maximum penalty is done heuristically and can be further optimized in future studies. Then, another outlook is the integration with error mitigation techniques [53–56], in order to improve the accuracy of the obtained results and scale the method to bigger physical systems.

In the end, we think that SPVQE should be taken in consideration for calculations regarding excited states, considering the straightforwardness of its implementation, its reliability and the accuracy improvements that it brought.

Appendix A. Improving constrained calculations

To improve both CVQE and SPVQE results in noisy and real quantum environments, we compute the expectation value of the Hamiltonian one last time after the algorithm has converged. In fact, even if we have the value of the cost function F and the penalty P correspondent to the best result found, the introduction of a penalty leads to a larger uncertainty.

We can show that with error propagation theory:

$$E = F - P \rightarrow \sigma_E = \sqrt{\sigma_F^2 + \sigma_P^2}. \quad (\text{A.1})$$

Measuring a last time the expectation value of the Hamiltonian, using the best computed parameters, give us a measure of the best energy with the error associated minimized, because we have:

$$E = F \rightarrow \sigma_E = \sigma_F < \sqrt{\sigma_F^2 + \sigma_P^2}. \quad (\text{A.2})$$

Appendix B. Robustness of SPVQE for different molecular systems

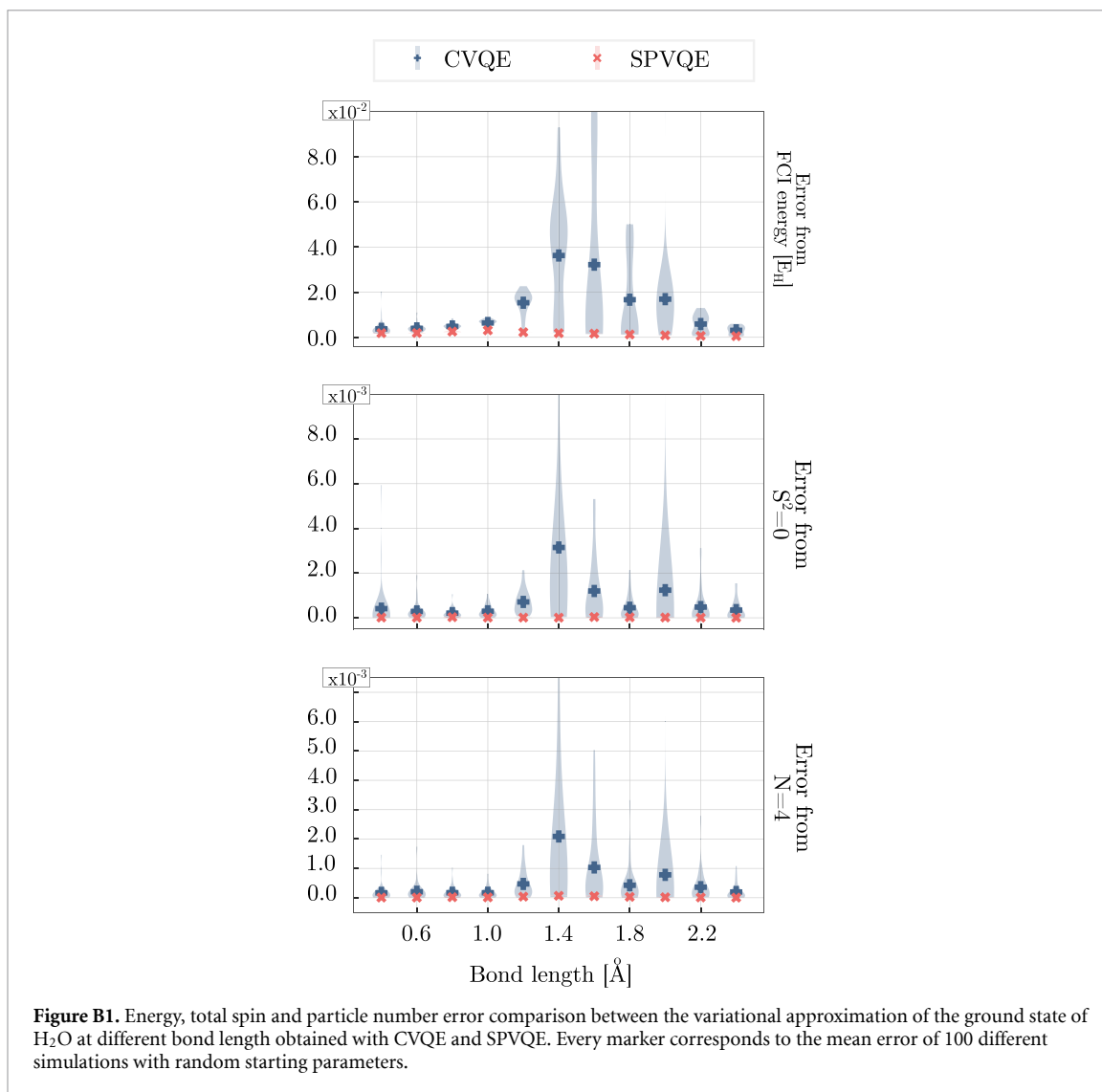
While in section 3.3 we presented the result for H_3^+ , we now show the same analysis for different molecules. This analysis shows that the robustness of SPVQE is not limited to the H_3^+ system. We simulated, in a noiseless environment, different molecules applying SPVQE and CVQE multiple times with different and random starting parameters.

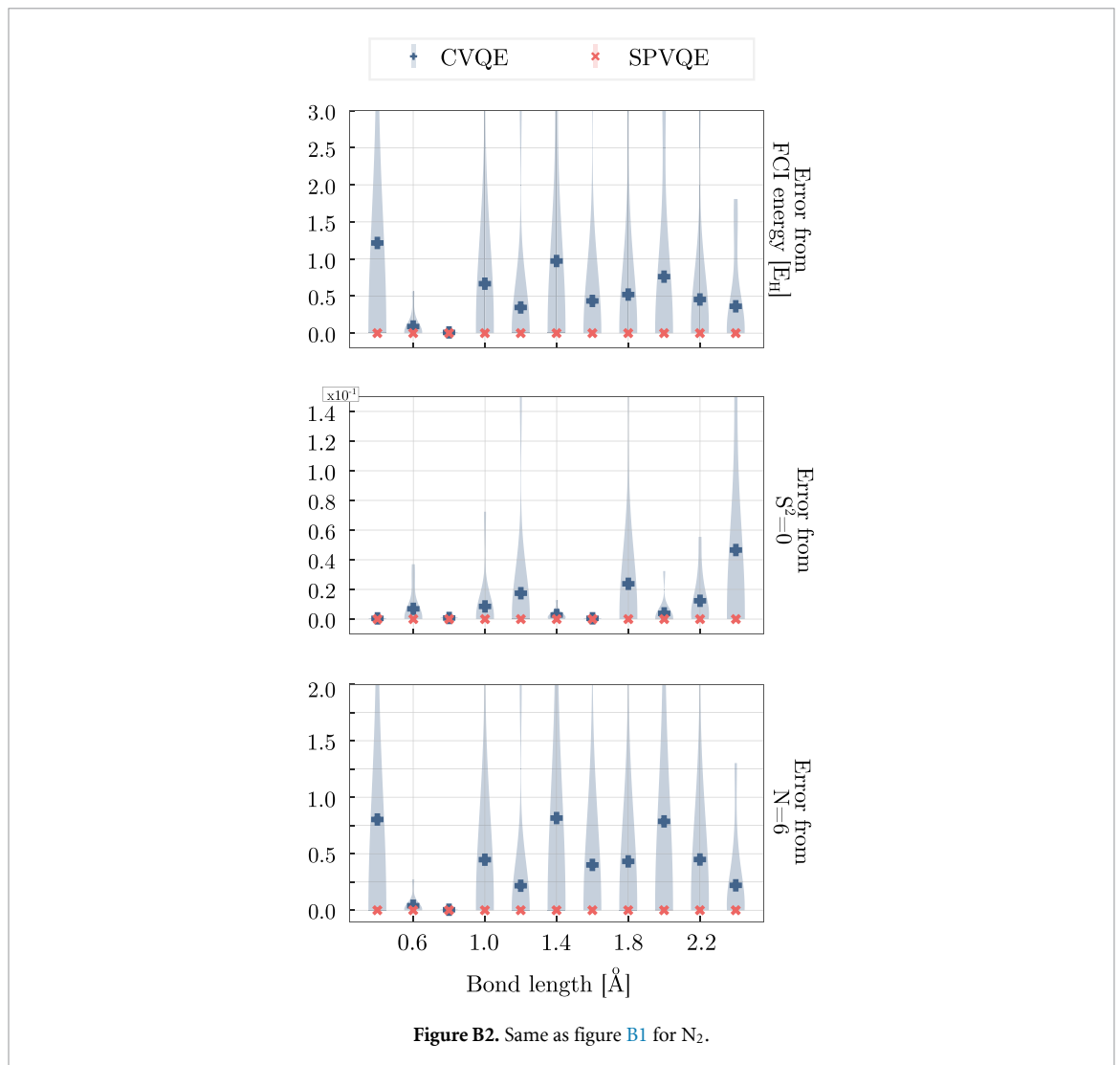
In particular, we studied the H_2O molecule for different bond lengths (we varied the position of one hydrogen atom in respect to $\text{H} - \text{O}$). To simulate a molecule with ten electrons, we froze the core orbitals, leaving just four particles to be placed in three molecular orbitals.

We highlight that results both of CVQE and SPVQE were obtained setting the same number of iteration for the optimizer.

We also repeated the same analysis for the N_2 molecule where we froze the core orbitals considering only six electrons in three molecular orbitals.

Results are shown in figures B1 and B2.





Appendix C. Noise simulations of SPVQE

We simulated H_3^+ dissociation profile considering a noise model imported from the *ibm_perth* IBM Quantum processor. Trihydrogen cation has 6 spin orbitals on the lowest shell: we therefore need a minimum of four qubits and a 16 parameters ansatz. For every method, to help the optimization, we used as starting ansatz parameters the optimal ones calculated for the last computation of that same method.

The results are presented in figure C1.

We can see that SPVQE outperforms both the standard VQE and the CVQE approach. The VQE fails to converge to the right physical state for bond lengths greater than 1.4 Å.

Compared to CVQE, the SPVQE approach converges to the desired value with higher precision both for total spin (the constrained operator) and energy.

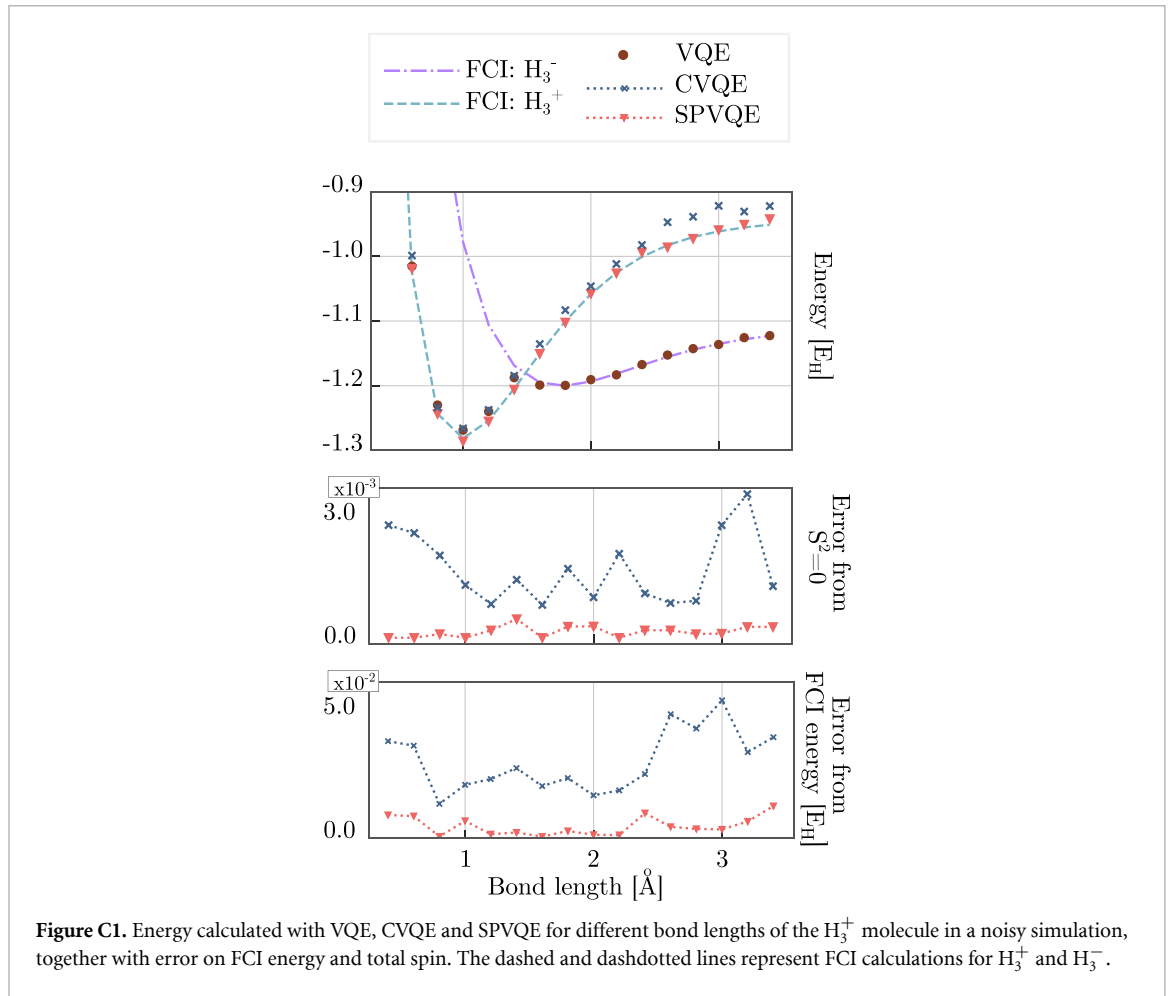


Table D1. Computational details for the molecules simulated in this paper. The bold H_3^+ corresponds to computations on hardware, where a shallower ansatz was used.

	Active electrons	Active orbitals	Qubits	D ansatz	Number of parameters
H_2	2 (all)	2 (all)	2	3	8
H_3^+	2 (all)	3 (all)	4	3	16
H_3^+	2 (all)	3 (all)	4	2	12
$Na-$	2	4	6	3	24
H_2O	4	3	4	3	16
N_2	6	3	4	3	16

Appendix D. Computational details for frozen-core approximation

For all the simulations and computations, we used the Qiskit package [48] (version 0.39.0 with qiskit-nature module at version 0.3.0) together with the PySCF package [57] (version 2.1.1).

To reduce computational burden we restricted the active space with the Qiskit ActiveSpaceTransformer. All the computed values, including frozen core energies and nuclear repulsion energies, are available on GitHub [49].

In table D1 we summarize some of the most important simulation details for every studied molecule. Here, bold symbols correspond to computations on hardware.

ORCID iDs

R Carobene <https://orcid.org/0000-0002-0579-3017>

S Barison <https://orcid.org/0000-0001-5842-1113>

A Giachero <https://orcid.org/0000-0003-0493-695X>

References

- [1] Ball P 2021 *Nature* **599** 542
- [2] Schindler P, Barreiro J T, Monz T, Nebendahl V, Nigg D, Chwalla M, Hennrich M and Blatt R 2011 *Science* **332** 1059–61
- [3] Kelly J et al 2015 *Nature* **519** 66–69
- [4] Ryan-Anderson C, Bohnet J G, Lee K, Gresh D, Hankin A, Gaebler J P, Francois D, Chernoguzov A, Lucchetti D, Brown N C, Gatterman T M, Halit S K, Gilmore K, Gerber J, Neyenhuis B, Hayes D and Stutz R P 2021 Realization of real-time fault-tolerant quantum error correction *Phys. Rev. X* **11** 041058
- [5] Egan L et al 2021 *Nature* **598** 281–6
- [6] Krinner S et al 2022 *Nature* **605** 669–74
- [7] Bharti K et al 2022 *Rev. Mod. Phys.* **94** 015004
- [8] Beckey J L et al 2020 *Phys. Rev. Res.* **4** 10488
- [9] Cerezo M et al 2020 *Nat. Rev. Phys.* **3** 625–44
- [10] Motta M, Sun C, Tan A T K, O'Rourke M J, Ye E, Minnich A J, Brandão F G S L and Chan G K-L 2019 *Nat. Phys.* **16** 205–10
- [11] Ollitrault P J, Kandala A, Chen C-F, Barkoutsos P K, Mezzacapo A, Pistoia M, Sheldon S, Woerner S, Gambetta J M and Tavernelli I 2020 *Phys. Rev. Res.* **2** 043140
- [12] Farhi E, Goldstone J and Gutmann S 2014 A quantum approximate optimization algorithm (arXiv:1411.4028)
- [13] Cao Y et al 2019 *Chem. Rev.* **119** 10856–915
- [14] Li Y and Benjamin S C 2017 *Phys. Rev. X* **7** 021050
- [15] Barison S, Vicentini F and Carleo G 2021 *Quantum* **5** 512
- [16] Avkhadiev A, Shanahan P E and Young R D 2019 *Phys. Rev. Lett.* **124** 080501
- [17] Cervia M J, Balantekin A B, Coppersmith S N, Johnson C W, Love P J, Poole C, Robbins K and Saffman M 2021 *Phys. Rev. C* **104** 024305
- [18] McClean J R, Romero J, Babbush R and Aspuru-Guzik A 2016 *New J. Phys.* **18** 023023
- [19] Peruzzo A, McClean J, Shadbolt P, Yung M-H, Zhou X-Q, Love P J, Aspuru-Guzik A and O'Brien J L 2014 *Nat. Commun.* **5** 1–7
- [20] O'Malley P J et al 2016 *Phys. Rev. X* **6** 031007
- [21] Tilly J et al 2022 The variational quantum eigensolver: a review of methods and best practices *Physics Reports* **986** 1–128
- [22] Colless J I et al 2018 *Phys. Rev. X* **8** 011021
- [23] Kandala A, Mezzacapo A, Temme K, Takita M, Brink M, Chow J M and Gambetta J M 2017 *Nature* **549** 242–6
- [24] Tang H L, Shkolnikov V, Barron G S, Grimsley H R, Mayhall N J, Barnes E and Economou S E 2021 *PRX Quantum* **2** 020310
- [25] Takeshita T, Rubin N C, Jiang Z, Lee E, Babbush R and McClean J R 2020 *Phys. Rev. X* **10** 011004
- [26] Yeter-Aydeniz K, Pooser R C and Siopsis G 2020 *npj Quantum Inf.* **6** 63
- [27] Tilly J, Jones G, Chen H, Wossnig L and Grant E 2020 *Phys. Rev. A* **102** 062425
- [28] Nakanishi K M, Mitarai K and Fujii K 2019 *Phys. Rev. Res.* **1** 033062
- [29] Ryabinkin I G, Genin S N and Izmaylov A F 2019 *J. Chem. Theory Comput.* **15** 249–55
- [30] Higgott O, Wang D and Brierley S 2019 *Quantum* **3** 156
- [31] Jones T, Endo S, McArdle S, Yuan X and Benjamin S C 2019 *Phys. Rev. A* **99** 062304
- [32] Danbo Z, Yuan Z H and Yin T 2022 Variational quantum eigensolvers by variance minimization *Chinese Physics B* **31** 12
- [33] Garcia-Saez A and Latorre J I 2018 Addressing hard classical problems with adiabatically assisted variational quantum eigensolvers (arXiv:1806.02287)
- [34] Jordan P and Wigner E P 1993 *The Collected Works of Eugene Paul Wigner* (Berlin: Springer)
- [35] Seeley J T, Richard M J and Love P J 2012 *J. Chem. Phys.* **137** 224109
- [36] Bravyi S B and Kitaev A Y 2002 *Ann. Phys., NY* **298** 210–26
- [37] Schuld M, Bergholm V, Gogolin C, Izaac J and Killoran N 2019 *Phys. Rev. A* **99** 032331
- [38] Mari A, Bromley T R and Killoran N 2021 *Phys. Rev. A* **103** 012405
- [39] Parrish R M, Hohenstein E G, McMahon P L and Martinez T J 2019 Hybrid quantum/classical derivative theory: analytical gradients and excited-state dynamics for the multistate contracted variational quantum eigensolver (arXiv:1906.08728)
- [40] Crooks G E 2019 Gradients of parameterized quantum gates using the parameter-shift rule and gate decomposition (arXiv:1905.13311)
- [41] Moll N, Fuhrer A, Staar P and Tavernelli I 2016 *J. Phys. A: Math. Theor.* **49** 295301
- [42] Bravyi S, Gambetta J M, Mezzacapo A and Temme K 2017 Tapering off qubits to simulate fermionic Hamiltonians (arXiv:1701.08213)
- [43] Barkoutsos P K et al 2018 *Phys. Rev. A* **98** 022322
- [44] Nocedal J and Wright S J 2006 *Numerical Optimization* 2nd edn (Berlin: Springer)
- [45] Kuroiwa K and Nakagawa Y O 2021 *Phys. Rev. Res.* **3** 13197
- [46] Virtanen P et al 2020 *Nat. Methods* **17** 261–72
- [47] Nakanishi K M, Fujii K and Todo S 2020 *Phys. Rev. Res.* **2** 43158
- [48] Aleksandrowicz G et al Qiskit contributors 2019 Qiskit: an open-source framework for quantum computing (<https://doi.org/10.5281/zenodo.2562111>)
- [49] Carobene R, Barison S and Giachero A 2023 SPVQE (available at: [SPVQE](https://github.com/CarobeneR/SPVQE))
- [50] Szabo A and Ostlund N S 1947 *Modern Quantum Chemistry* (New York: Dover Publications, INC.)
- [51] Kitaev A Y, Shen A H and Vyalyi M N 2002 *Classical and Quantum Computation* (Providence, RI: American Mathematical Society)
- [52] Cross A W, Bishop L S, Sheldon S, Nation P D and Gambetta J M 2019 *Phys. Rev. A* **100** 032328
- [53] Giurgica-Tiron T, Hindy Y, LaRose R, Mari A and Zeng W J 2020 Digital zero noise extrapolation for quantum error mitigation 2020 *IEEE Int. Conf. on Quantum Computing and Engineering (QCE)* (IEEE)
- [54] Temme K, Bravyi S and Gambetta J M 2017 *Phys. Rev. Lett.* **119** 180509
- [55] Pokharel B, Anand N, Fortman B and Lidar D A 2018 *Phys. Rev. Lett.* **121** 220502
- [56] Kandala A, Temme K, Córcoles A D, Mezzacapo A, Chow J M and Gambetta J M 2019 *Nature* **567** 491–5
- [57] Sun Q et al 2018 *Wiley Interdiscip. Rev.-Comput. Mol. Sci.* **8** e1340